knockout mouse after E10.5 somitogenesis, but not prior to E10.5. It is reasonable to assume that the requirement of Notch clock oscillation by *Lfng* changes during somitogenesis and is lesser at later stages, as now suggested by a number of studies (Shifley et al., 2008; Stauber et al., 2009).

Acknowledgements
We thank Ryoichiro Kageyama (Kyoto University) for providing the *Hes7* promoter and enhancer cassette, Aya Satoh, Nobuo Sasaki and Yusuke Okubo (National Institute of Genetics) for animal care and the preparation of embryo samples and Mariko Ikumi, Eriko Ikeno and Shinobu Watanabe (National Institute of Health Sciences) for technical assistance. This work was supported in part by Grants-in-Aid for Scientific Research on Priority Areas, Dynamics of Extracellular Environments, and by the National BioResource Project from the Ministry of Education, Culture, Sports, Science and Technology, Japan.

Competing interests statement
The authors declare no competing financial interests.

Supplementary material
Supplementary material for this article is available at
http://dev.biologists.org/lookup/suppl/doi:10.1242/dev.044545/-/DC1

References
Aulehla, A. and Johnson, R. L. (1999). Dynamic expression of lunatic fringe suggests a link between notch signaling and an autonomous cellular oscillator driving somite segmentation. *Dev. Biol.* **207**, 49-61.
Aulehla, A., Wehrle, C., Brand-Saberi, B., Kemler, R., Gossler, A., Kanzler, B. and Herrmann, B. G. (2003). Wnt3a plays a major role in the segmentation clock controlling somitogenesis. *Dev. Cell* **4**, 395-406.
Aulehla, A., Wiegraebe, W., Baubet, V., Wahl, M. B., Deng, C., Taketo, M., Lewandoski, M. and Pourquie, O. (2008). A beta-catenin gradient links the clock and wavefront systems in mouse embryo segmentation. *Nat. Cell Biol.* **10**, 186-193.
Barrantes, I. B., Elia, A. J., Wunsch, K., Hrabe de Angelis, M. H., Mak, T. W., Rossant, J., Conlon, R. A., Gossler, A. and de la Pompa, J. L. (1999). Interaction between Notch signalling and Lunatic fringe during somite boundary formation in the mouse. *Curr. Biol.* **9**, 470-480.
Bessho, Y., Hirata, H., Masamizu, Y. and Kageyama, R. (2003). Periodic repression by the bHLH factor Hes7 is an essential mechanism for the somite segmentation clock. *Genes Dev.* **17**, 1451-1456.
Cole, S. E., Levorse, J. M., Tilghman, S. M. and Vogt, T. F. (2002). Clock regulatory elements control cyclic expression of Lunatic fringe during somitogenesis. *Dev. Cell* **3**, 75-84.
Dale, K. J. and Pourquie, O. (2000). A clock-work somite. *BioEssays* **22**, 72-83.
Delfini, M. C., Dubrulle, J., Malapert, P., Chal, J. and Pourquie, O. (2005). Control of the segmentation process by graded MAPK/ERK activation in the chick embryo. *Proc. Natl. Acad. Sci. USA* **102**, 11343-11348.
Dequeant, M. L. and Pourquie, O. (2008). Segmental patterning of the vertebrate embryonic axis. *Nat. Rev. Genet.* **9**, 370-382.
Dequeant, M. L., Glynn, E., Gaudenz, K., Wahl, M., Chen, J., Mushegian, A. and Pourquie, O. (2006). A complex oscillating network of signaling genes underlies the mouse segmentation clock. *Science* **314**, 1595-1598.
Evrard, Y. A., Lun, Y., Aulehla, A., Gan, L. and Johnson, R. L. (1998). lunatic fringe is an essential mediator of somite segmentation and patterning. *Nature* **394**, 377-381.
Feller, J., Schneider, A., Schuster-Gossler, K. and Gossler, A. (2008). Noncyclic Notch activity in the presomitic mesoderm demonstrates uncoupling of somite compartmentalization and boundary formation. *Genes Dev.* **22**, 2166-2171.
Horikawa, K., Ishimatsu, K., Yoshimoto, E., Kondo, S. and Takeda, H. (2006). Noise-resistant and synchronized oscillation of the segmentation clock. *Nature* **441**, 719-723.
Lewis, J. (2003). Autoinhibition with transcriptional delay: a simple mechanism for the zebrafish somitogenesis oscillator. *Curr. Biol.* **13**, 1398-1408.
McGrew, M. J., Dale, J. K., Fraboulet, S. and Pourquie, O. (1998). The lunatic fringe gene is a target of the molecular clock linked to somite segmentation in avian embryos. *Curr. Biol.* **8**, 979-982.
Morales, A. V., Yasuda, Y. and Ish-Horowicz, D. (2002). Periodic Lunatic fringe expression is controlled during segmentation by a cyclic transcriptional enhancer responsive to notch signaling. *Dev. Cell* **3**, 63-74.
Morimoto, M., Takahashi, Y., Endo, M. and Saga, Y. (2005). The Mesp2 transcription factor establishes segmental borders by suppressing Notch activity. *Nature* **435**, 354-359.
Nakajima, Y., Morimoto, M., Takahashi, Y., Koseki, H. and Saga, Y. (2006). Identification of Epha4 enhancer required for segmental expression and the regulation by Mesp2. *Development* **133**, 2517-2525.
Niwa, Y., Masamizu, Y., Liu, T., Nakayama, R., Deng, C. X. and Kageyama, R. (2007). The initiation and propagation of Hes7 oscillation are cooperatively regulated by Fgf and notch signaling in the somite segmentation clock. *Dev. Cell* **13**, 298-304.
Oginuma, M., Niwa, Y., Chapman, D. L. and Saga, Y. (2008). Mesp2 and Tbx6 cooperatively create periodic patterns coupled with the clock machinery during mouse somitogenesis. *Development* **135**, 2555-2562.
Ozbudak, E. M. and Lewis, J. (2008). Notch signalling synchronizes the zebrafish segmentation clock but is not needed to create somite boundaries. *PLoS Genet.* **4**, e15.
Palmeirim, I., Henrique, D., Ish-Horowicz, D. and Pourquie, O. (1997). Avian hairy gene expression identifies a molecular clock linked to vertebrate segmentation and somitogenesis. *Cell* **91**, 639-648.
Riedel-Kruse, I. H., Muller, C. and Oates, A. C. (2007). Synchrony dynamics during initiation, failure, and rescue of the segmentation clock. *Science* **317**, 1911-1915.
Sakai, K. and Miyazaki, J. (1997). A transgenic mouse line that retains Cre recombinase activity in mature oocytes irrespective of the cre transgene transmission. *Biochem. Biophys. Res. Commun.* **237**, 318-324.
Shifley, E. T., Vanhorn, K. M., Perez-Balaguer, A., Franklin, J. D., Weinstein, M. and Cole, S. E. (2008). Oscillatory lunatic fringe activity is crucial for segmentation of the anterior but not posterior skeleton. *Development* **135**, 899-908.
Stauber, M., Sachidanandan, C., Morgenstern, C. and Ish-Horowicz, D. (2009). Differential axial requirements for lunatic fringe and Hes7 transcription during mouse somitogenesis. *PLoS One* **4**, e7996.
Takahashi, Y., Koizumi, K., Takagi, A., Kitajima, S., Inoue, T., Koseki, H. and Saga, Y. (2000). Mesp2 initiates somite segmentation through the Notch signalling pathway. *Nat. Genet.* **25**, 390-396.
Takahashi, Y., Inoue, T., Gossler, A. and Saga, Y. (2003). Feedback loops comprising Dll1, Dll3 and Mesp2, and differential involvement of Psen1 are essential for rostrocaudal patterning of somites. *Development* **130**, 4259-4268.
Takahashi, Y., Yasuhiko, Y., Kitajima, S., Kanno, J. and Saga, Y. (2007). Appropriate suppression of Notch signaling by Mesp factors is essential for stripe pattern formation leading to segment boundary formation. *Dev. Biol.* **304**, 593-603.
Wahl, M. B., Deng, C., Lewandoski, M. and Pourquie, O. (2007). FGF signaling acts upstream of the NOTCH and WNT signaling pathways to control segmentation clock oscillations in mouse somitogenesis. *Development* **134**, 4033-4041.
Watanabe, T., Sato, Y., Saito, D., Tadokoro, R. and Takahashi, Y. (2009). EphrinB2 coordinates the formation of a morphological boundary and cell epithelialization during somite segmentation. *Proc. Natl. Acad. Sci. USA* **106**, 7467-7472.
Yasuhiko, Y., Haraguchi, S., Kitajima, S., Takahashi, Y., Kanno, J. and Saga, Y. (2006). Tbx6-mediated Notch signaling controls somite-specific Mesp2 expression. *Proc. Natl. Acad. Sci. USA* **103**, 3651-3656.
Zhang, N. and Gridley, T. (1998). Defects in somite formation in lunatic fringe-deficient mice. *Nature* **394**, 374-377.

Industrial Health 2010, **48**, 783–795 **Original Article**

Pulmonary Toxicity of Intratracheally Instilled Multiwall Carbon Nanotubes in Male Fischer 344 Rats

Shigetoshi AISO[1]*, Kazunori YAMAZAKI[1], Yumi UMEDA[1], Masumi ASAKURA[1], Tatsuya KASAI[1], Mitsutoshi TAKAYA[2], Tadao TOYA[2], Shigeki KODA[2], Kasuke NAGANO[1], Heihachiro ARITO[1] and Shoji FUKUSHIMA[1]

[1]Japan Bioassay Research Center, Japan Industrial Safety and Health Association, 2445 Hirasawa, Hadano, Kanagawa 257-0015, Japan
[2]National Institute of Occupational Safety and Health, 6–21–1 Nagao, Tama-ku, Kawasaki 214-8585, Japan

Received July 23, 2009 and accepted January 8, 2010

Abstract: In order to assess pulmonary toxicity of multiwall carbon nanotubes (MWCNT), male F344 rats were intratracheally instilled with MWCNT suspension at a dose of 40 or 160 μg/head or α-quartz particles as a positive control at a dose of 160 μg/head and sacrificed for lung histopathology and bronchoalveolar lavage (BAL) fluid analyses on Day 1, 7, 28 or 91 after instillation. Well-dispersed MWCNT brought about dose- or time-dependent changes in lung weight, total proteins, albumin, lactate dehydrogenase and alkaline phosphatase in the BAL fluid, and pulmonary lesions including inflammation, Type II cell hyperplasia, microgranulomas and fibrosis. Phagocytosed and free forms of MWCNT were found in both bronchiolar and alveolar spaces. MWCNT deposition in the bronchus-associated lymphoid tissue gradually increased after instillation. Persistent infiltration of macrophages, transient infiltration of inflammatory cells primarily composed of neutrophils, microgranulomas associated with macrophages engulfing MWCNT, Type II cell hyperplasia and fibrosis with alveolar wall thickening as well as number of multinucleated alveolar macrophages increased dose-dependently. The MWCNT-induced lesions were more potent on Day 91 than the α-quartz-induced ones at an equal mass dose. The present results for intratracheally instilled MWCNT were extrapolated to potential inhalation exposure of humans to MWCNT at workplaces based on several assumptions.

Key words: Multiwall carbon nanotube, Neutrophils, Alveolar macrophages, Granuloma, Fibrosis, Alveolar wall thickening, Type II cell hyperplasia, Multinucleated cell

Introduction

Carbon nanotubes (CNT) have been reported to possess unusually excellent electrical, mechanical and thermal properties, and thus have many potential applications in electronics, computers, aerospace, and the medical and pharmaceutical industries[1, 2]. According to an article in Nature[3], Smalley predicted that in time, millions of tons of CNT will be produced worldwide every year. Yearly production volumes of single-wall carbon nanotubes (SWCNT) and multiwall carbon nanotubes (MWCNT) in Japan were estimated to be 0.1 and 60 tons, respectively[4]. With the rapid increase in industrial production of CNT, much concern has been raised over the health consequences for workers who are exposed to SWCNT or MWCNT in their occupational settings. Neither epidemiological nor medical case studies have been reported on the health consequences of CNT-exposed workers. However, the toxicity of CNT has been examined by exposing experimental animals to CNT by intraperitoneal injection, intratracheal instillation, pharyngeal aspiration or by inhalation. The reported findings of these *in vivo* toxicity studies of CNT

*To whom correspondence should be addressed.
E-mail: s-aiso@jisha.or.jp

included mesotheliomas in *p*53 gene-deficient mice[5] and intact male F344 rats[6], asbestos-like pathogenicity in female mice[7], induction of inflammation and fibrosis of the lung in mice[8–11] and rats[12, 13], inflammation and oxidative stress in the lungs of vitamin E-deficient mice[14], granulomas in the lungs of rats and mice[5–15], induction of apoptosis in the absence of inflammation in the rat lung[16], and systemic immunosuppression in mice[17]. Inflammation was reported to occur in the mouse lung after intratracheal instillation[8–11, 14] but not after inhalation exposure to MWCNT[17]. The pulmonary toxicity of MWCNT was reported to alter with pretreatment of MWCNT[18]. Mutation of k-*ras* gene locus in the lungs of mice exposed by inhalation to SWCNT[11], and positive clastogenicity and aneugenicity of MWCNT[19] in Type II pneumocytes of female rats given intratracheally instilled MWCNT have also been reported. In addition to positive mutagenicity, oxidative stress and pulmonary lesions such as inflammation, hyperplasia and fibrosis are important determinants in carcinogenesis[20, 21].

The present study was designed to examine dose- and time-dependent relationships between deposition of MWCNT and its extent in the lung, and pulmonary toxic responses such as inflammation, granuloma and fibrosis in rats intratracheally instilled with MWCNT. The affected lungs were examined for both lung histopathology and biochemical and cytological analyses of bronchoalveolar lavage (BAL) fluid, with reference to the lung lesions and their severities induced by intratracheally instilled α-quartz as a positive control. The results of the dose characteristics of MWCNT in the suspension were accepted for publication in this Journal as a separate paper[22].

Materials and Methods

Animals

Male F344/DuCrlCrlj rats were purchased from Charles River Japan, Inc. (Kanagawa, Japan) at the age of 11 wk. The animals were quarantined and acclimated for 2 wk, then housed individually in stainless steel wire-mesh hanging cages (170W × 294D × 176H mm) under controlled environmental conditions (temperature of 24 ± 2°C and a relative humidity of 55 ± 10% with 15 to 17 air changes/h). Fluorescent lighting was controlled automatically to provide a 12-h light/dark cycle. All rats had free access to sterilized water and γ-irradiation-sterilized commercial pellet diet (CRF-1, Oriental Yeast Co., Ltd., Tokyo, Japan). The animals were cared for in accordance with the Guide for the Care and Use of Laboratory Animals[23], and the present study was approved by the ethics committee of the Japan Bioassay Research Center (JBRC).

Test substances

MWCNT was kindly supplied by MITSUI & Co. Ltd. (MWCNT-7, Lot No. 061220, Tokyo, Japan). α-Quartz in the form of crystalline silica (MIN-U-SIL 5) was purchased from US. Silica Co. (WV, USA), and the nominal size of α-quartz particles was 1.7 μm in median diameter. MWCNT and α-quartz were used in the present study as produced; i.e., without being purified or further sieved. Since neither MWCNT nor α-quartz is water-soluble or wettable, these test substances were suspended in phosphate-buffered saline (PBS) containing 0.1% Tween 80 as a colloidal dispersant and subjected to ultrasonication for 20 min with an ultrasonic homogenizer (VP-30S, 20 kHz, 300 W, TAITEC Co., Ltd, Tokyo, Japan). The size distribution of the MWCNT in the suspension was measured by both a dynamic light scattering size measurement (DLS) and scanning electron microscopic (SEM) observation[22]. Briefly, the DLS measurement showed that the median hydrodynamic diameter of MWCNT in the suspension after 20-min ultrasonication ranged below 1.0 μm. The SEM observation revealed that the mean length and width of the MWCNT fibers were 5.0 μm and 88 nm, respectively, and that fibers longer than 5.0 μm occupied 38.9% of the total fibers counted. The MWCNT was found to contain 4,400 ppm (wt/wt) iron, 48 ppm chromium and 17 ppm nickel by graphite furnace atomic absorption spectrometric analysis, and these levels of metals were considered not to elicit any positive pulmonary responses[22]. Measurement of endotoxin levels in the PBS-Tween 80 suspending MWCNT or α-quartz was commissioned to Japan SLC, Ltd. (Tokyo, Japan). The levels of endotoxin in the PBS-Tween 80 suspending MWCNT, α-quartz and in the vehicle PBS-Tween 80 were below 0.9 pg/ml, indicating the absence of contamination of MWCNT or α-quartz with bacteria.

Intratracheal instillation

Immediately before intratracheal instillation, the ultrasonicated suspension of MWCNT, α-quartz or vehicle solution was further subjected to additional ultrasonication for 30s with a sonicator (US-2, AS ONE Co., Ltd., Tokyo, Japan). After inhalational anesthetization with isoflurane gas (Forane, Abbott Japan Co., Ltd., Tokyo, Japan), the suspension of MWCNT or α-quartz in PBS-Tween 80 (0.3 ml) or the vehicle solution (0.3 ml) was intratracheally instilled, using a microspray cannula of Intratracheal Aerosolizer (1A-1B, PennCentury, Inc., USA). Successful delivery of the instilled MWCNT into lungs was confirmed by observing both a wheezing sound and rapid recovery from anesthesia with neither abnormal behavior nor negative health outcomes at the time of instillation. The animals treated with the MWCNT, α-quartz suspension or the vehicle solution recovered quickly after anesthesia without any behavioral or negative health outcomes.

Experimental design

A total of 192 rats were used for the study of MWCNT toxicity, while 96 rats were used for the positive control study of α-quartz toxicity, consisting of 48 α-quartz-dosed rats and 48 vehicle-dosed rats for a negative control. After quarantine and acclimation for 2 wk, the animals were divided by stratified randomization into two MWCNT-dosed, one α-quartz-dosed positive and one vehicle-dosed negative control group, each consisting of 16 rats/group, at each of the time points for sacrifice. The two experimental groups received MWCNT at doses of 40 and 160 μg/head (equivalent to 160 or 640 μg/kg body weight) by intratracheal instillation. The dose levels of MWCNT were selected, in consideration of doses which would allow extrapolation to potential exposure of humans to MWCNT in real workplaces. The positive control group was intratracheally instilled with α-quartz at a dose of 160 μg/head, while the negative control group received PBS-Tween 80 by intratracheal instillation. MWCNT- and vehicle-dosed animals were sacrificed on Day 1, 7, 28 or 91 following intratracheal instillation, whereas the α-quartz-dosed animals were not sacrificed on Day 7. Mean and SD of body weights were 262.2 ± 11.7 g for all the rats immediately before intratracheal instillation.

Lung fixation and histopathology

In order to prepare for light microscopic examination, 8 rats/group were sacrificed at each time point by exsanguination from the jugular vein under pentobarbital anesthesia, and the trachea was ligated. The organs and tissues were fixed by perfusion with physiological saline and subsequently 10% neutral buffered formalin, and embedded in paraffin. Slices of the left lung, 5 μm thick, were cut along the longitudinal axis of the main bronchus. The slices were stained with hematoxylin and eosin (H & E) or Masson's trichrome.

Deposition of MWCNT was semi-quantitatively evaluated for the extent to which the instilled MWCNT was deposited in the bronchiolar space, alveolar space, alveolar wall and bronchus-associated lymphoid tissue (BALT). The severity grade of histopathological changes was scored semi-quantitatively for infiltration of inflammatory cells primarily composed of neutrophils, hyperplasia of Type II pneumocytes, microgranuloma and fibrosis. The extent of MWCNT deposition or the severity grade of histopathological change was scored, according to the following criteria by microscopic observation of H & E- or Masson's trichrome-stained lung tissues. Score 1, termed "slight", indicates that slight MWCNT deposition or histopathological change was observed in a limited part of the area. Score 2, termed "moderate", indicates that slight MWCNT deposition or histopathological change was observed in a large part of the area or that moderate MWCNT deposition or histopathological change was observed in a limited part of the area. Score 3, termed "marked", indicates that moderate MWCNT deposition or histopathological change was observed in a large part of the area or that marked MWCNT deposition or histopathological change was observed in a limited part of the area. These evaluations were performed by a panel of 3 pathologists certified by the Japanese Society of Toxicologic Pathology.

Measurement of lung weight and biochemical and cytological analyses of BAL fluid

The experimental and control groups of 8 rats each were euthanized under pentobarbital anesthesia. First, the right bronchus was tied, then the right lung was taken out and weighed after lavaging the left lung. The left lung was lavaged 3 times with 7 ml of physiological saline solution, and the wash-out was collected. After the BAL fluid was centrifuged at 10,000 rpm and 4°C for 10 min, aliquots of the acellular supernatant were used for biochemical analysis. Total proteins (TP), albumin, lactate dehydrogenase (LDH) and alkaline phosphatase (ALP) were measured by conventional biochemical methods. TP was chosen as an indicator for maintenance of alveolo-capillary permeability, and LDH and ALP were used as indicators for membrane integrity of pneumocytes and Type II epithelial cells, respectively. The BAL fluid was centrifuged with a cytospin (Cytospin4, Thermo Scientific, USA), and the cellular elements were stained with May-Grünwald-Giemsa. The numbers of mononucleated and multinucleated alveolar macrophages were counted for a total of 1,000 cells under a light-microscope. The presence or absence of MWCNT in the macrophages was also examined.

Statistics

Absolute lung weight and biochemical parameters in the BAL fluid were analyzed by Student's *t*-test, and the number of multinucleated alveolar macrophages in the BAL fluid was analyzed by Dunnett's multiple comparison test, using statistics software (SPSS Japan Inc., Tokyo, Japan). Differences between groups at $p<0.05$ were considered significant.

Results

Clinical signs and body and lung weights

Neither death nor overt clinical signs were observed in any MWCNT-, α-quartz-dosed or control animals. As shown in Fig. 1, body weights of rats given 40 or 160 μg MWCNT or 160 μg α-quartz were not significantly different from those of the two control groups at any time point after intratracheal instillation. The absolute lung weights of the two MWCNT-dosed groups were significantly greater than those of the vehicle control on days 1, 7 and 91 after instillation (Fig. 2). On the other hand, there were no statistically significant differences between the absolute lung weights of the α-quartz-dosed group and the vehicle control (Fig. 2).

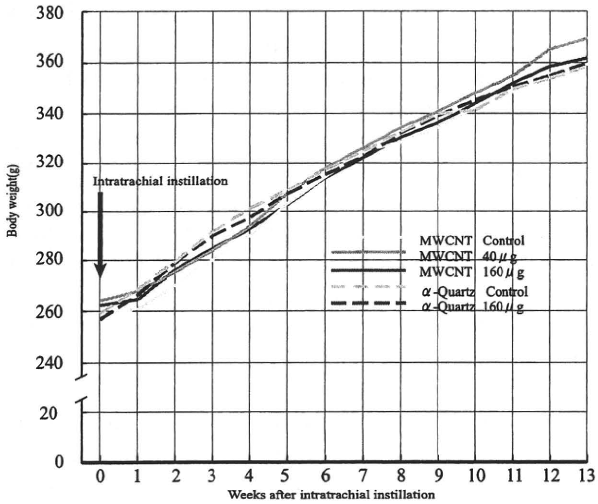

Fig. 1. Temporal changes in body weight of rats which received intratracheal instillation of MWCNT at a dose of 40 or 160 μg, or α-quartz at a dose of 160 μg or the vehicle PBS-Tween 80 as positive and negative controls.

Pulmonary deposition of MWCNT

Table 1 shows the pulmonary deposition of MWCNT, and the extent to which MWCNT was deposited in the lung tissues, on different days after instillation. MWCNT deposition was abundant in the bronchiolar and alveolar spaces. The extent of MWCNT deposition decreased in the order of the alveolar space, alveolar wall and BALT. The free form of MWCNT decreased more rapidly in the bronchiolar and alveolar spaces than the phagocytosed form, whereas the phagocytosed form of MWCNT was observed throughout the 91-d post-exposure period. Although MWCNT deposition in the alveolar wall was not observed on Day 1, the deposition of MWCNT and its extent increased on Day 28 and slightly decreased on Day 91. Notably, BALT exhibited a tendency of MWCNT deposition and its extent gradually increased with time after instillation, although MWCNT deposition was not observed on Day 1 in either BALT or the alveolar wall. The extent to which MWCNT was deposited in these lung tissues was milder in the 40-μg-dosed group than in the 160-μg-dosed one.

Lung histopathology

Table 2 summarizes the time- and dose-dependent changes and severity of pulmonary toxic responses in the rats given MWCNT by intratracheal instillation at doses of 40 and 160 μg, with reference to those seen in the 160-μg α-quartz group, the positive control, and the vehicle PBS group, the negative control. Dose-dependent infiltration of macrophages in the alveolar space persisted throughout the 91-d post-exposure period, whereas infiltration of inflammatory cells composed primarily of neutrophils was found to occur only on Day 1 after dosing 160 μg MWCNT. Alveolar macrophages without nucleus or with pycnotic nuclei were often found in the bronchiolar space and alveolar

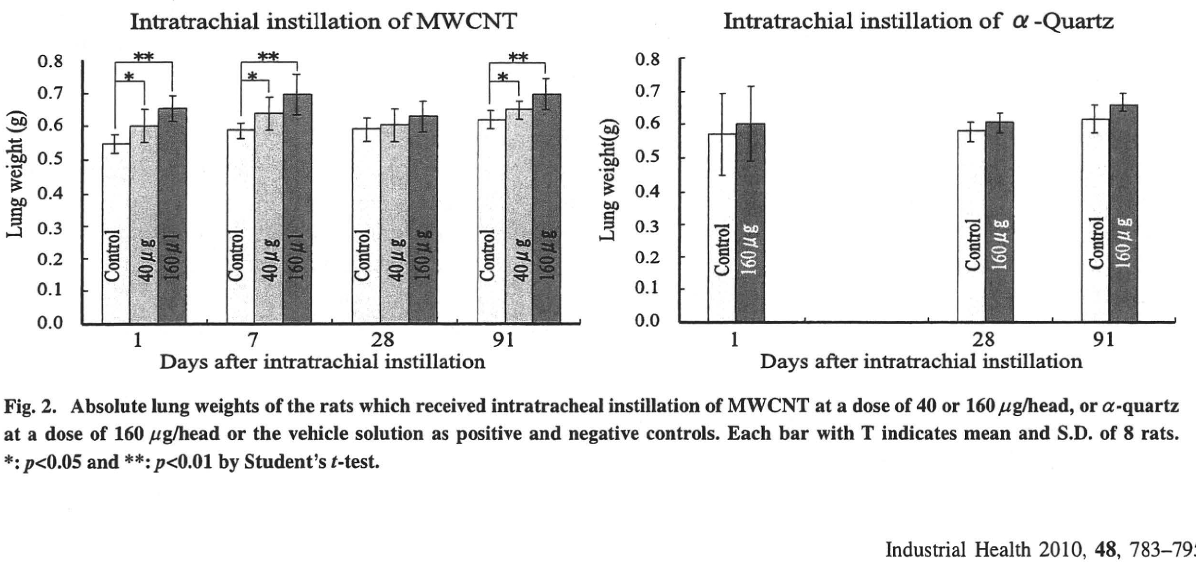

Fig. 2. Absolute lung weights of the rats which received intratracheal instillation of MWCNT at a dose of 40 or 160 μg/head, or α-quartz at a dose of 160 μg/head or the vehicle solution as positive and negative controls. Each bar with T indicates mean and S.D. of 8 rats. *: $p<0.05$ and **: $p<0.01$ by Student's t-test.

Table 1. Temporal changes in pulmonary deposition of intratracheally instilled MWCNT at a dose of 40 or 160 μg in the rats sacrificed on different days after the instillation

Dose of MWCNT(/rat)		40 µg				160 µg			
Days after instillation		1	7	28	91	1	7	28	91
No. of rats examined		8	8	8	8	8	8	8	8
Bronchiolar space									
Non-phagocytosed	Total[a]	8	4	2	0	8	8	2	1
	Slight	8	4	2	0	7	8	2	1
	Moderate	0	0	0	0	1	0	0	0
Phagocytosed by alveolar macrophages	Total[a]	8	6	7	4	8	8	8	6
	Slight	8	6	7	4	7	8	8	6
	Moderate	0	0	0	0	1	0	0	0
Alveolar space									
Non-phagocytosed	Total[a]	8	0	0	0	8	6	0	0
	Slight	8	0	0	0	0	6	0	0
	Moderate	0	0	0	0	8	0	0	0
Phagocytosed by alveolar macrophages	Total[a]	8	8	8	8	8	8	8	8
	Slight	0	3	0	7	0	0	0	0
	Moderate	8	5	8	1	0	0	1	0
	Marked	0	0	0	0	8	8	7	8
Alveolar wall	Total[a]	0	1	8	4	0	8	8	8
	Slight	0	1	8	3	0	0	1	2
	Moderate	0	0	0	1	0	8	7	6
Bronchus-associated lymphoid tissue	Total[a]	0	3	3	8	0	1	6	8
	Slight	0	3	3	6	0	1	6	4
	Moderate	0	0	0	2	0	0	0	4

[a]:Total number of animals bearing the lesions.
Scoring of grade of pulmonary deposition of MWCNT was given in Materials and Methods.

Table 2. Pulmonary lesions induced by intratracheal instillation of MWCNT at a dose of 40 or 160 μg or α-quartz at a dose of 160 μg in rats sacrificed on different days after the instillation

Dose(/rat)		MWCNT 40 µg				MWCNT 160 µg				α-Quartz 160 µg				Vehicle control			
Days after instillation		1	7	28	91	1	7	28	91	1	7	28	91	1	7	28	91
No. of rats examined		8	8	8	8	8	8	8	8	8	n.e.	8	8	8	8	8	8
Infiltration of alveolar macrophages	Total[a]	8	8	8	8	8	8	8	8	8	-	6	4	0	0	0	0
	Slight	0	3	0	7	0	0	0	0	8		6	4	0	0	0	0
	Moderate	8	5	8	1	0	0	1	0	0		0	0	0	0	0	0
	Marked	0	0	0	0	8	8	7	8	0		0	0	0	0	0	0
Infiltration of inflammatory cells	Total[a]	0	0	0	0	8	0	0	0	6	-	0	0	0	0	0	0
	Slight	0	0	0	0	0	0	0	0	6		0	0	0	0	0	0
	Moderate	0	0	0	0	8	0	0	0	0		0	0	0	0	0	0
Hyperplasia of Type II pneumocytes	Total[a]	0	1	7	4	0	8	8	8	0	-	0	3	0	0	0	0
	Slight	0	1	6	4	0	8	2	5	0		0	3	0	0	0	0
	Moderate	0	0	1	0	0	0	6	3	0		0	0	0	0	0	0
Microgranuloma	Total[a]	0	0	0	0	0	7	6	7	0	-	0	0	0	0	0	0
	Slight	0	0	0	0	0	6	1	2	0		0	0	0	0	0	0
	Moderate	0	0	0	0	0	1	5	5	0		0	0	0	0	0	0
Fibrosis	Total[a]	0	0	0	7	0	0	8	8	0	-	1	7	0	0	0	0
	Slight	0	0	0	7	0	0	8	0	0		1	7	0	0	0	0
	Moderate	0	0	0	0	0	0	0	8	0		0	0	0	0	0	0

Data of vechicle control group are shown for the MWCNT-dosed groups. The vechicle control data for the α-quartz-dosed groups are not shown, since the control group wsa the same as the vechicle control group of the MWCNT dosed group. Scoring of severity grade of the pulmonary lesions is given in Materials and Methods. n.e.: Not examined. [a]:Total number of animals bearing the lesions.

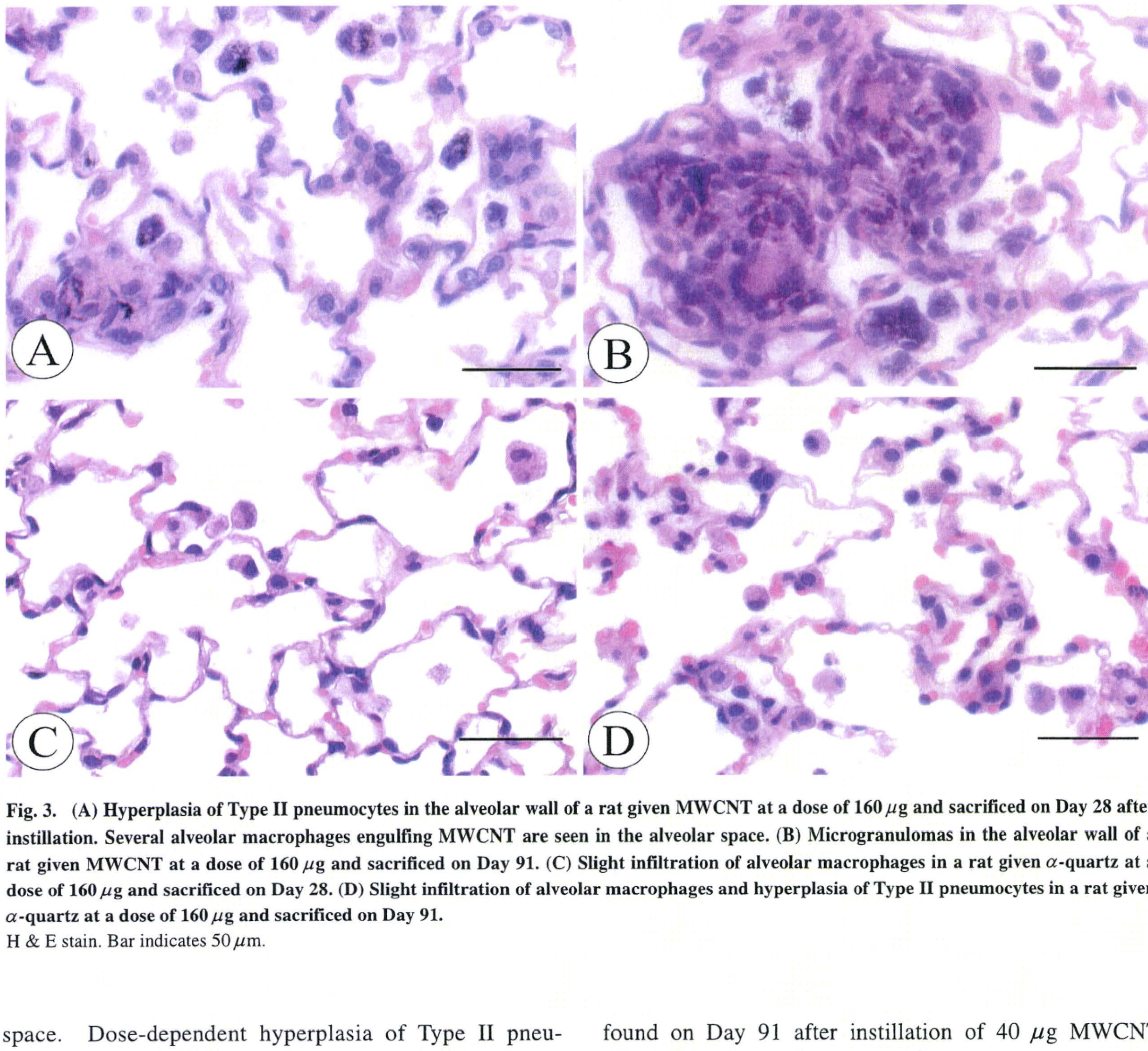

Fig. 3. (A) Hyperplasia of Type II pneumocytes in the alveolar wall of a rat given MWCNT at a dose of 160 μg and sacrificed on Day 28 after instillation. Several alveolar macrophages engulfing MWCNT are seen in the alveolar space. (B) Microgranulomas in the alveolar wall of a rat given MWCNT at a dose of 160 μg and sacrificed on Day 91. (C) Slight infiltration of alveolar macrophages in a rat given α-quartz at a dose of 160 μg and sacrificed on Day 28. (D) Slight infiltration of alveolar macrophages and hyperplasia of Type II pneumocytes in a rat given α-quartz at a dose of 160 μg and sacrificed on Day 91.
H & E stain. Bar indicates 50 μm.

space. Dose-dependent hyperplasia of Type II pneumocytes (Fig. 3A) was observed persistently throughout the 91-d post-exposure period, although hyperplasia did not occur on Day 1. Notably, microgranulomas with diameters up to 150 μm, which were primarily composed of alveolar macrophages engulfing MWCNT (Fig. 3B), were found to occur multifocally only in the 160 μg-dosed group. Some of those macrophages were multinucleated. Although microgranulomas were not seen on Day 1, the number of rats bearing microgranulomas and their severities as expressed by the number lesions in a designated area tended to increase along the time-course of the 91-d post-exposure period. The microgranulomas found in the 160 μg-dosed group were occasionally associated with fibrosis of moderate grade of severity, as evidenced by alveolar wall thickening due to collagen deposition which was stained blue with Masson's trichrome (Fig. 4A). However, slight fibrosis in the absence of overt microgranulomas was found on Day 91 after instillation of 40 μg MWCNT (Fig. 4B). The pulmonary toxic responses to α-quartz at a dose of 160 μg were characterized by persistent infiltration of macrophages (Fig. 3C and 3D), transient infiltration of inflammatory cells primarily composed of neutrophils, Type II cell hyperplasia (Fig. 3D) and alveolar wall thickening diagnosed as slight fibrosis, all of which were less severe in their severities than the pulmonary toxic responses to MWCNT on an equal mass basis (Table 2). Alveolar wall thickening as slight fibrosis observed on Day 91 after dosing 160 μg α-quartz (Fig. 4C) was similar in grade of severity to that induced on Day 91 after dosing 40 μg MWCNT. No histopathological changes were observed in either bronchi or bronchioles in any treated group. No overt histopathological changes in MWCNT-induced lesions were found in the visceral pleura.

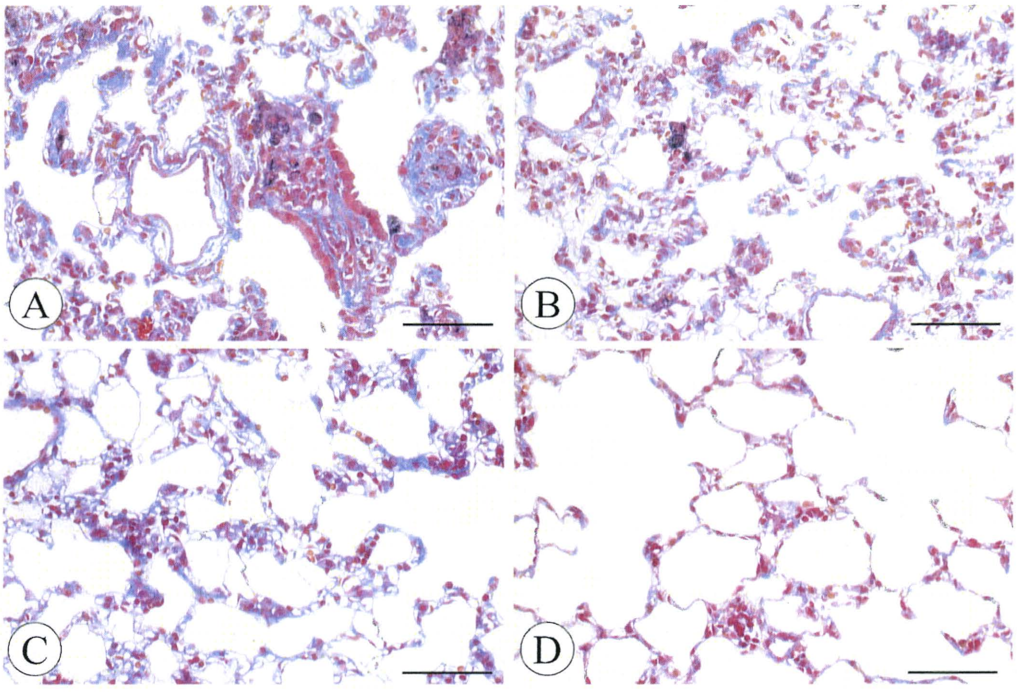

Fig. 4. Fibrosis in the alveolar wall of the rats given MWCNT at a dose of 160 μg (A), 40 μg (B) or α-quartz at a dose of 160 μg (C), and sacrificed on Day 91. A control rat given the vehicle solution at an equal volume and sacrificed on Day 91 (D).
Masson's trichrome stain. Bar indicates 100 μm.

Biochemical and cytological analyses of BAL fluid

TP and albumin contents markedly increased with dose of MWCNT on Day 1. This trend attenuated toward control levels thereafter but persisted significantly until Day 91 (Fig. 5). Temporal changes in both LDH and ALP activities took the same trend as those of TP and albumin. Intratracheal instillation of 160 μg α-quartz induced a significant increase in the contents of proteins and albumin, and LDH and ALP activities on Days 1, 28 and 91 after instillation. Although the biochemical responses to α-quartz on Day 1 were less severe than those to MWCNT, the response magnitudes of α-quartz on Day 91 were similar to those of MWCNT at an equal dose of 160 μg.

Light microscopic examination revealed that a small fraction of alveolar macrophages in the BAL fluid were multinucleated, engulfing the entangled MWCNT fibers in the cytoplasm (inset of Fig. 6). The number of multinucleated alveolar macrophages in the BAL fluid of MWCNT-dosed rats increased significantly and dose-dependently on Day 7 through 91, except on Day 1 (Fig. 6).

Discussion

In the present study, intratracheal instillation of MWCNT suspended in the PBS-Tween 80 at doses of 40 and 160 μg/rat was found to produce dose- and time-dependent changes in incidences and severities of pulmonary lesions, lung weight and biochemical and cytological parameters of BAL fluid.

In the separate paper[22], we reported that the 20-min and additional 30-s ultrasonication and intratracheal instillation of MWCNT suspended in PBS containing 0.1% Tween 80 allowed good dispersion of MWCNT fibers in the suspension at the time of intratracheal instillation with a microspray cannula. Besides, the well-dispersed MWCNT fibers were partly engulfed by alveolar macrophages in the alveolar area of MWCNT-dosed rats sacrificed on Day 1 after instillation, suggesting the occurrence of frustrated phagocytosis or incomplete phagocytosis, as proposed by Poland *et al.*[7] and Hubbs *et al.*[24], respectively. Therefore, the results suggest that the tissue around the alveolar area is exposed to well-dispersed MWCNT fibers in the absence of large MWCNT aggregates. Entangled or densely-packed MWCNT fibers in the alveolar interstitium were observed occasionally on Day 91 after instillation. We consider this type of MWCNT to have been formed in the interstitium through re-agglomeration of the MWCNT fibers which had been released from the necrotic or apoptotic macrophages, since in the present

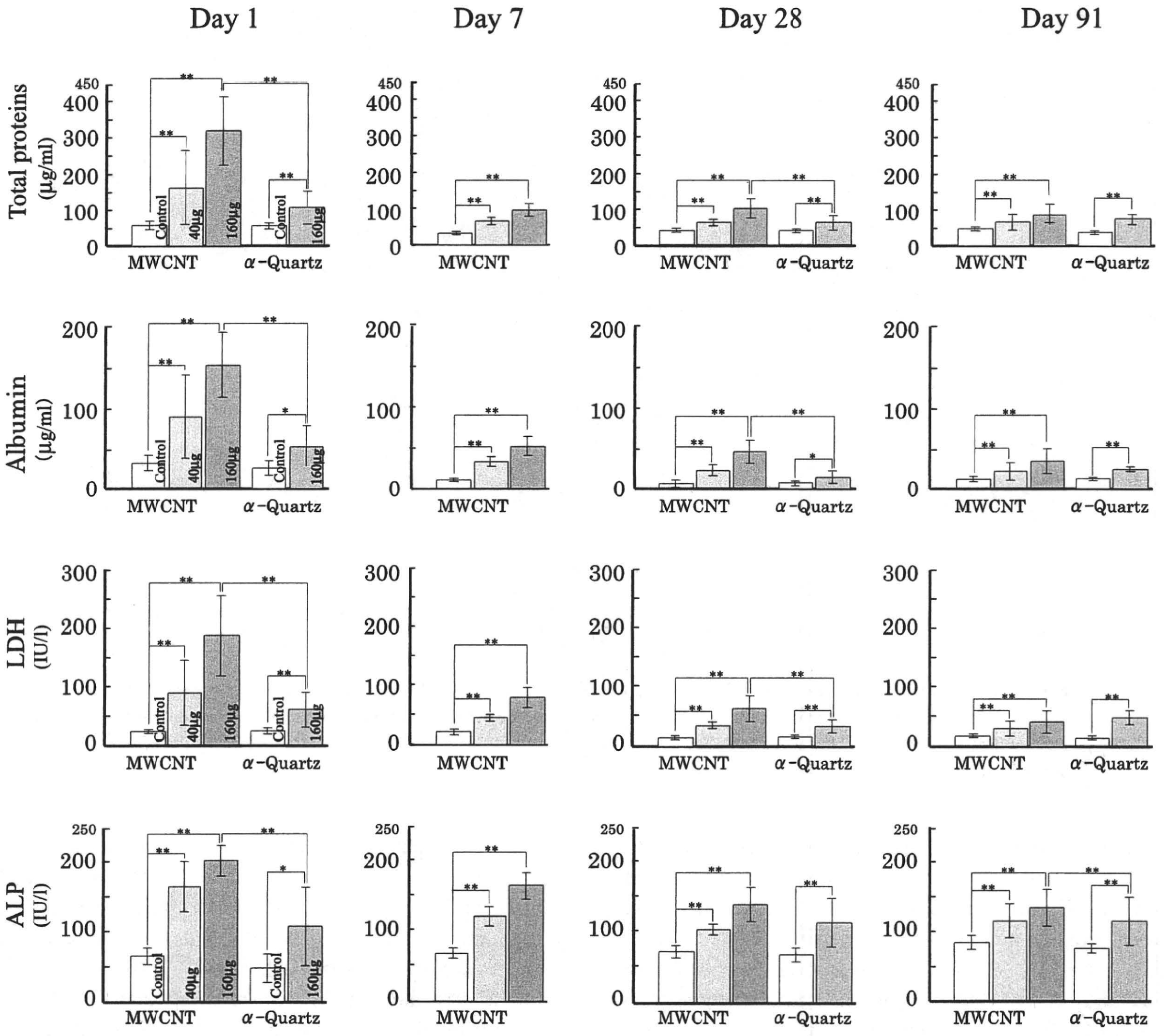

Fig. 5. Contents of total proteins, albumin, LDH and ALP in BAL fluid of the rats which received intratracheal instillation of MWCNT at doses of 40 or 160 μg, or α-quartz at a dose of 160 μg, and were sacrificed on different days after instillation.

A bar with T indicates mean and SD of 8 rats. *: $p<0.05$ and **: $p<0.01$ by Student's t-test.

study densely-packed MWCNT was not found in the instilling suspension or in the bronchiolar and alveolar spaces on Day 1 after instillation.

Light microscopic observation of pulmonary deposition of MWCNT revealed that the non-phagocytosed (free) form of MWCNT in the bronchiolar and alveolar spaces was cleared faster than the phagocytosed form, and that the phagocytosed form of MWCNT in the bronchiolar and alveolar spaces and the MWCNT deposition in the alveolar wall and BALT, except on Day 1, were persistent throughout the 91-d post-exposure period. Notably, deposition of MWCNT and its extent in the BALT tended to increase along the time course of the 91-d post-exposure period. Morrow[25] reported that there are two different pathways of pulmonary lymphatic drainage, the pleural drainage and the "deep-set" drainage. BALT belongs to the "deep-set" drainage of periarterial, perivenous and peribronchiolar lympth vessels for clearance of fibers deposited in the interstitium. Pulmonary lymphatic drainage is reported to be much slower in clearing particles and fibers deposited in the interstitium than in the mucociliary escalator[26–30]. Therefore, the present result of a gradual increase in BALT deposition of MWCNT could be accounted by slow clearance of interstitially deposited MWCNT through pulmonary lympthatic drainage unlike the fast clearance of non-phagocytosed MWCNT fibers in the bronchiolar and alveolar spaces through the mucociliary escalator. Persistence of MWCNT fibers in the alveolar interstitium might allow sufficient time for migration of the

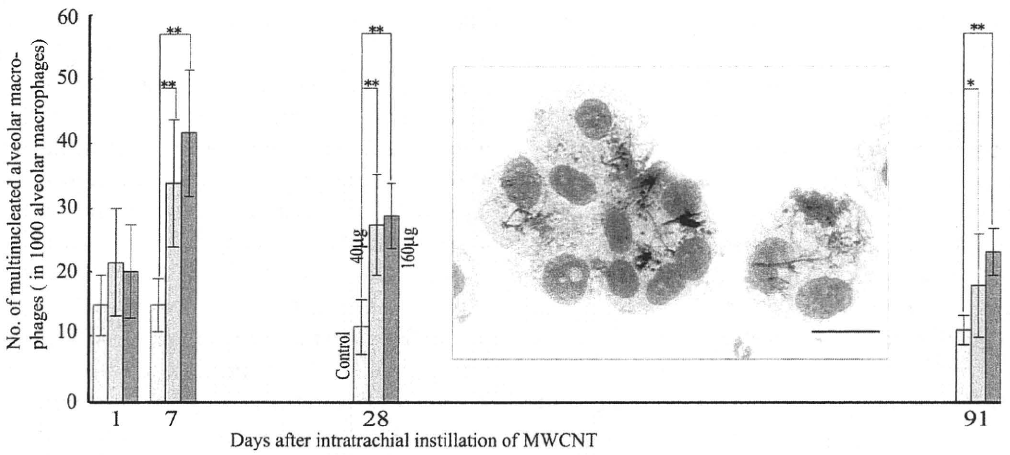

Fig. 6. Number of multinucleated alveolar macrophages in BAL fluid of the rats which received intratracheal instillation of MWCNT at a dose of 40 or 160 μg and were sacrificed on Day 1, 7, 28 or 91 after the instillation. Data indicates means and SDs of 8 rats.

*: p<0.05 and **: p<0.01 by Dunnett's multiple comparison test. Inset shows multinucleated alveolar macrophages engulfing MWCNT in the cytoplasm in the BAL fluid from a rat given 160 μg MWCNT and sacrificed on Day 7 after the instillation. May-Grünwald-Giemsa stain. Bar indicates 25 μm.

fibers through the pulmonary lymphatic pathway adjacent to the pleural cavity. Deposition of MWCNT in the pulmonary lymphatics such as BALT suggests that the dispersed MWCNT fibers might migrate from the alveolar interstitium to the pleura and exert asbestos-like lung pathogenicity in the pleural cavity, as hypothesized by Poland *et al.*[7] The mean length and width of MWCNT fibers used in the present study were 5.0 μm and 88 nm, respectively, with an averaged aspect ratio of 57, and fibers longer than 5 μm were found to occupy 38.9% of total fibers[22], suggesting a similarity in size and shape of MWCNT and asbestos fibers. Peritoneal and intrascrotal administrations of MWCNT fibers having an equal length and width as those used in the present study are reported to have induced peritoneal mesotheliomas in male p53 gene-deficient mice[5] and intact male F344 rats[6], respectively. Intratracheally instilled fibers of chrysotile asbestos are reported to translocate to the pleural cavity in rats[31], which corresponds to the human parietal pleura as a preferential target of asbestos-related pathology[32].

In the present study, intratracheal instillation of MWCNT at a high dose of 160 μg was found to multifocally induce microgranulomas with diameters up to 150 μm, which were primarily composed of alveolar macrophages engulfing dispersed MWCNT fibers. Besides, the microgranuloma was occasionally associated with fibrosis which was evidenced by alveolar wall thickening due to collagen deposition stained blue with Masson's trichrome. A granulomatous response in close association with inflammation has been addressed in rodents receiving an agglomerated, less dispersed form of SWCNT or MWCNT at high doses by intratracheal instillation or pharyngeal aspiration. Lam *et al.*[8] observed that a single intratracheal instillation of SWCNT in mice induced persistent epitheloid granulomas and interstitial inflammation. However, Warheit *et al.*[15] reported that intratracheal instillation of SWCNT in rats given a bolus dose of agglomerated SWCNT induced multifocal granulomas centered around SWCNT, but they ascribed the granulomatous response as non-specific outcome. It was demonstrated that pharyngeal aspiration of agglomerated, less dispersed SWCNT in mice induced granulomatous lesions associated with dense SWCNT aggregate as well as inflammation and diffuse interstitial fibrosis with alveolar wall thickening[9]. However, well-dispersed SWCNT did not produce granulomatous lesions but caused more extensive interstitial fibrosis than less-dispersed SWCNT fibers[10]. Muller *et al.*[12] showed biochemical and histological lines of evidence for inflammation and fibrosis in the lungs of rats given MWCNT by intratracheal instillation. It can be inferred, therefore, that the microgranulomas and slight to moderate fibrosis with alveolar wall thickening found in the present study might have been caused by the persistence of MWCNT in the alveolar wall and interstitium, resulting in persistent infiltration of macrophages which would release proinflammatory and profibrogenic cytokines during phagocytosis.

Hyperplasia of Type II pneumocytes found in the present study is considered to reflect either increased number of Type II cells due to Type I cell injury or proliferation of Type II cells, or both. This histopathological finding is compatible with the significantly increased ALP activity in the BAL fluid throughout the 91-d post-exposure period, since enhanced ALP activity has been reported to reflect secretory activity of Type II pneumocytes[15, 33]. The present result is also consistent with the findings of Shvedova *et al.* that pharyngeal aspiration of SWCNT in mice increased the immunofluorescentce of cytokeratins 8/18 and markers of Type II epithelial cells in the alveolus, and the number of cells expressing cytoplasmic lamellar bodies in TEM sections. Hyperplasia of Type II pneumocytes and persistent infiltration of macrophages throughout the 91-d post-exposure period, together with the significant increases in total proteins and albumin in the BAL fluid until Day 91, might actually reflect impaired integrity of the alveolar space-capillary function such as gas exchange, resulting in increased alveolo-capillary permeability of proteins and Type II cell hyperplasia, probably due to injury of Type I pneumocytes by MWCNT.

In the present study, the number of multinucleated macrophages engulfing MWCNT in the BAL fluid increased significantly and dose-dependently on Days 7 and 91. This finding is consistent with previously published results that multinucleated macrophages were observed after intraperitoneal injection of MWCNT in mice[5–7] and intratracheal instillation of SWCNT in rats[15]. The formation of multinucleated alveolar macrophages engulfing MWCNT fibers can be hypothesized to result from interference with the mitotic spindle or steric blocking of cytokinesis by MWCNT fibers, or both. This hypothesis seems to be supported by two previously reported findings with SWCNT[11, 13]. Mangum *et al.*[13] reported that a small fraction of alveolar macrophages in the BAL fluid of SWCNT-exposed rats was bridged by intercellular carbon structures that extended into the cytoplasm of each macrophage. Shvedova *et al.*[11] suggested possible interference with the mitotic spindle on the basis of their histopathological observation of an anaphase bridge in a dividing macrophage containing SWCNT in the lung of mice exposed by inhalation to SWCNT aerosol. Further evidence in support of this was provided by the formation of polyploidy by sterical blocking of cytokinesis in cultured LLC-MK_2 cells exposed *in vitro* to long crocidolite asbestos fibers[34]. Since the MWCNT fibers used in the present study were long and thin[22], like asbestos fibers, well-dispersed in the lung tissues and biopersistent, MWCNT might act upon the lung like asbestos fibers, as suggested by Poland *et al*[7].

The pulmonary lesions induced by 160 μg α-quartz were characterized by slight but statistically significant increases in the biochemical parameters of the BAL fluid on Day 1 as compared with the marked lesions induced by 160 μg MWCNT, and by persistent infiltration of macrophages, and slight grade of Type II cell hyperplasia and fibrosis with alveolar wall thickening on Day 91. It has been reported that nodular changes in the interstitium, lipoproteinosis and fibrosis are induced by intratracheal instillation of α-quartz to rats at higher dose levels than 1 mg[15, 35] or by repeated inhalation exposure of rats to α-quartz at 15 mg/m^3 for 60 d[36]. However, no such lesions except fibrosis with alveolar wall thickening were found to occur in the lung of 160 μg quartz-dosed rats. Therefore, the comparison between MWCNT and α-quartz findings suggests that MWCNT-induced lesions are more potent on Day 91 than the α-quartz-induced ones on an equal mass basis, although the biochemical responses of BAL fluid to MWCNT were similar in magnitude on Day 91 than those to α-quartz.

Animal data of exposure concentration-response relationships from inhalation exposure are more relevant to the health risk assessment of workers exposed to MWCNT than those from intratracheal instillation, because inhalation exposure is a primary route of exposure for humans handling MWCNT in workplaces. Besides, intratracheal instillation of MWCNT is non-physiological, and involves invasive delivery which bypasses the upper respiratory tract, usually at a dose and/or dose rate substantially greater than that which would have occurred in inhalation. An excessive lung burden due to insoluble and low-toxic particles termed "lung overload" has been reported to impair alveolar macrophage clearance which in turn leads to increased retention and accumulation of particles in the lung, resulting in development of chronic inflammation and fibrosis[37, 38]. The dose levels that cause the lung overload in rats vary among the related reports. Morrow[37] reported that the level of dust burden causing overloading appears to be greater than 1–2 mg of persistently retained dust in the lungs of F344 rats, whereas Driscoll *et al.*[39] recommended that intratracheal doses below approximately 100 μg/rat be used to minimize the interference of clumping and localized inflammatory responses to insoluble particles. Drew *et al.*[40] reported that single boluses of glass fibers at high doses (2 and 20 mg/rat) produced artifactual granulomatous lesions in the rat lung, whereas repeated exposure to low doses of fiber (0.1 mg/rat) resulted in a fiber distribution and response similar to that after inhalation. Taking these reports[37–40] into consideration, a single dose of 160 μg/rat for intratracheal instillation of MWCNT, as used in the present study, would minimize the lung overload and induce unambiguous pulmonary toxic responses to MWCNT. In particular, the low dose of 40 μg/rat would not cause the lung overload.

In the present study, a single intratracheal instillation of well-dispersed MWCNT at a dose of 40 μg/rat was found to induce slight but persistent changes in the biochemical parameters in BAL fluid and histopathological lung lesions including Type II cell hyperplasia and slight fibrosis with alveolar wall thickening in the absence of overt microgranulomas. Assuming respiratory rate of 561 ml/min/kg body weight[41] for a rat weighing 0.25 kg and a lung deposition efficiency of 11%[42] for MWCNT in the alveolar area, the intratracheally instilled dose of 40 μg/rat can be estimated to be equivalent to the lung burden resulting from inhalation exposure of rats to MWCNT aerosol at 5.4 mg/m^3 for 8 h. This estimated airborne level was found to coincide well with the current OSHA's permissible exposure limit (PEL) of 5 mg/m^3 TWA (respirable fraction) for graphite particles[43].

No data for CNT concentrations in workplace air have been reported to date, except for the measurement[44] of the peak airborne concentration of respirable dust during handling of SWCNT in a real workplace, 53 μg/m^3 by Maynard *et al.* Assuming that a worker would breathe air laden with MWCNT aerosol at an average of 53 μg/m^3 during an 8-h shift of light work with a minute ventilation of 0.02 m^3/min[45], and assuming that 11% of respirable MWCNT aerosol with an aerodynamic diameter of 0.70 μm would be deposited in the alveolar area[46], 56 μg of MWCNT would be to deposited on the worker's alveolar epithelial surface area. Assuming even distribution of 56 μg of inhaled MWCNT and 40 μg of intratracheally instilled MWCNT over the alveolar surface area of human and rat lungs, respectively, and normalizing to the equivalent alveolar surface area in the human (143 m^2/lung) and rat (0.392 m^2/lung) from the published morphometric analysis[47], the amount of MWCNT deposited on the unit alveolar surface area would be 0.39 μg/m^2 for humans and 102 μg/m^2 for rats. With additional assumptions of both no clearance of MWCNT depositing on the surface of alveoli and equal susceptibility of the alveolar epithelium per unit area to MWCNT for humans and rats, the burden of MWCNT on the unit alveolar surface area of the 40 μg MWCNT-instilled rat can be estimated to be equivalent to the alveolar burden of MWCNT of a worker who would breathe air laden with MWCNT aerosol at an average concentration of 53 μg/m^3 for 8 h/day and 260 workdays. Therefore, it is considered that the low dose level of MWCNT used in the present study is relevant to potential occupational exposure to MWCNT, suggesting a need for the establishment of an occupational standard for airborne CNT aerosol in workplace air.

In conclusion, single intratracheal instillations of well-dispersed MWCNT at doses of 40 and 160 μg/rat were found to induce histopathological, cytological and biochemical changes in the lung tissues and BAL fluid. These MWCNT-induced pulmonary lesions were time- and dose-dependent and more potent than those induced by α-quartz on an equal mass basis. The present results with intratracheally instilled MWCNT were discussed with regared to extrapolation to potential inhalation exposure of humans to MWCNT at workplaces based on several assumptions.

Acknowledgements

The authors are deeply indebted to Dr. Haruhiko Sakurai, Technical Advisor, Occupational Health Research and Development Center, Japan Industrial Safety and Health Association for his fruitful discussion on risk assessment of MWCNT. We also thank Ms. Hitomi Kondo, Misae Saito, Mrs. Hirokazu Kano, Masaaki Suzuki, Dr. Michiharu Matsumoto, Dr. Tetsuya Takeuchi and Dr. Hirokazu Okuda for their excellent technical assistance with the BAL analyses, intratracheal instillation, statistical analysis, and animal care and clinical observation. The present study was supported in part by a Grant-in-Aid for Scientific Research from the Ministry of Health, Labour and Welfare of Japan.

References

1) Martin CR, Kohli P (2003) The emerging field of nanotube biotechnology. Nat Rev Drug Discov **2**, 29–37.
2) Ajayan PM, Charlier JC, Rinzler AG (1999) Carbon nanotubes: from macromolecules to nanotechnology. Proc Natl Acad Sci USA **96**, 14199–200.
3) Ball P (2001) Roll up for the revolution. Nature **414**, 142–4.
4) Toray Corporate Business Research, INC. Report on the survey of production and use of nanomaterials in Japan, -Fy 2007-. http://www.mhlw.go.jp/shingi/2008/04/dl/s0404-3c.pdf. Accessed July 21, 2009 (in Japanese).
5) Takagi A, Hirose A, Nishimura T, Fukumori N, Ogata A, Ohashi N, Kitajima S, Kanno J (2008) Induction of mesothelioma in p53+/– mouse by intraperitoneal application of multi-wall carbon nanotube. J Toxicol Sci **33**, 105–16.
6) Sakamoto Y, Nakae D, Fukumori N, Tayama K, Maekawa A, Imai K, Hirose A, Nishimura T, Ohashi N, Ogata A (2009) Induction of mesothelioma by a single intrascrotal administration of multi-wall carbon nanotube in intact male Fischer 344 rats. J Toxicol Sci **34**, 65–76.
7) Poland CA, Duffin R, Kinloch I, Maynard A, Wallace

WAH, Seaton A, Stone V, Brown S, MacNee W, Donaldson K (2008) Carbon nanotubes introduced into the abdominal cavity of mice show asbestos-like pathogenicity in a pilot study. Nature Nanotechnology **3**, 423–8.

8) Lam CW, James JT, McCluskey R, Hunter RL (2004) Pulmonary toxicity of single-wall carbon nanotubes in mice 7 and 90 days after intratracheal instillation. Toxicol Sci **77**, 126–34.

9) Shvedova AA, Kisin ER, Mercer R, Murray AR, Johnson VJ, Potapovich AI, Tyurina YY, Gorelik O, Arepalli S, Schwegler-Berry D, Hubbs AF, Antonini J, Evans DE, Ku BK, Ramsey D, Maynard A, Kagan VE, Castranova V, Baron P (2005) Unusual inflammatory and fibrogenic pulmonary responses to single-walled carbon nanotubes in mice. Am J Physiol Lung Cell Mol Physiol **289**, L698–L708.

10) Mercer RR, Scabilloni J, Wang L, Kisin E, Murray AR, Schwegler-Berry D, Shvedova AA, Castranova V (2008) Alteration of deposition pattern and pulmonary response as a result of improved dispersion of aspirated single-walled carbon nanotubes in a mouse model. Am J Physiol Lung Cell Mol Physiol **294**, L87–L97.

11) Shvedova AA, Kisin E, Murray AR, Johnson VJ, Gorelik O, Arepalli S, Hubbs AF, Mercer RR, Keohavong P, Sussman N, Jin J, Yin J, Stone S, Chen BT, Deye G, Maynard A, Castranova V, Baron PA, Kagan VE (2008) Inhalation vs. aspiration of single walled carbon nanotubes in C57BL/6 mice: inflammation, fibrosis, oxidative stress, and mutagenesis. Am J Pysiol Lung Cell Mol Physiol **295**, L552–L65.

12) Muller J, Huaux F, Moreau N, Misson P, Heilier JF, Delos M, Arras M, Fonseca A, Nagy JB, Lison D (2005) Respiratory toxicity of multi-wall carbon nanotubes. Toxicol Appl Pharmacol **207**, 221–31.

13) Mangum JB, Turpin EA, Antao-Menezes A, Cesta MF, Bermudez E, Bonner JC (2006) Single-walled carbon nanotube (SWCNT)-induced interstitial fibrosis in the lungs of rats is associated with increased levels of PDGF mRNA and the formation of unique intercellular carbon structures that bridge alveolar macrophages *in Situ*. Particle Fibre Toxicol **3**, 1–13.

14) Shvedova AA, Kisin ER, Murray AR, Gorelik O, Arepalli S, Castranova V, Young S-H, Gao F, Tyurina YY, Oury TD, Kagan VE (2007) Vitamine E deficiency enhances pulmonary inflammatory response and oxidative stress induced by single-walled carbon nanotubes in C57BL/6 mice. Toxicol Appl Pharmacol **221**, 339–48.

15) Warheit DB, Laurence BR, Reed KL, Roach DH, Reynolds GAM, Webb TR (2004) Comparative pulmonary toxicity assessment of single-wall carbon nanotubes in rats. Toxicol Sci **77**, 117–25.

16) Elgrabli D, Abella-Gallart S, Robidel F, Rogerieux F, Boczkowski J, Lacroix G (2008) Induction of apoptosis and absence of inflammation in rat lung after intratracheal instillation of multiwalled carbon nanotubes. Toxicol **253**, 131–6.

17) Mitchell LA, Gao J, Wal RV, Gigliotti A, Burchiel SW, McDonald JD (2007) Pulmonary and systemic immune response to inhaled multiwalled carbon nanotubes. Toxicol Sci **100**, 203–14.

18) Muller J, Huaux F, Fonseca A, Nagy JB, Moreau N, Delos M, Raymundo-Piñero E, Béguin F, Kirsch-Volders M, Fenoglio I, Fubini B, Lison D (2008) Structural defects play a major role in the acute lung toxicity of multiwall carbon nanotubes: toxicologucal aspects. Chem Res Toxicol **21**, 1698–705.

19) Muller J, Decordier I, Hoet PH, Lombaert N, Thomassen L, Huaux F, Lison D, Kirsch-Volders M (2008) Clastogenic and aneugenic effects of multi-wall carbon nanotubes in epithelial cells. Carcinogenesis **29**, 427–33.

20) Hubbard R, Venn A, Lewis S, Britton J (2000) Lung cancer and cryptogenic fibrosing alveolitis. A population-based cohort study. Am J Respir Crit Care Med **161**, 5–8.

21) Fraire AE, Greenberg SD (1973) Carcinoma and diffuse interstitial fibrosis of lung. Cancer **31**, 1078–86.

22) Takaya M, Serita F, Yamazaki K, Aiso S, Kubota H, Asakura M, Ikawa N, Nagano K, Arito H, Fukushima S (2010) Characteristics of multiwall carbon nanotubes for an intratracheal instillation study with rats. Ind Health **48**, 452–9.

23) National Research Council (1996) Guide for the care and use of laboratory animals. National Academy Press, Institute of Laboratory Animal Resources Commission on Life Sciences, NRC, Washington, DC.

24) Hubbs A, Mercer RR, Coad JE, Barrelli LA, Willard PA, Sriram K, Wolfarth M, Castranova V, Porter D (2009) Persistent pulmonary inflammation, airway mucous metaplasia and migration of multiwalled carbon nanotubes from the lung after subchronic exposure. The Toxicologist (48th Annual Meeting of SOT) 457.

25) Morrow PE (1972) Lymphatic drainage of the lung in dust clearance. Ann NY Acad Sci **200**, 46–65.

26) Lee KP, Trochimowicz HJ, Reinhardt CF (1985) Transmigration of titanium dioxide (TiO_2) particles in rats after inhalation exposure. Exp Mol Pathol **42**, 331–43.

27) Takahashi S, Patrick G (1987) Patterns of lymphatic drainage to individual thoracic and cervical lymph nodes in the rat. Lab Anim **21**, 31–4.

28) Lehnert BE, Valdez YE, Stewart CC (1986) Translocation of particles to the tracheobronchial lympth nodes after lung deposition: kinetics and particle-cell relationships. Exp Lung Res **10**, 245–66.

29) Ferin J, Oberdörster G, Penney DP (1992) Pulmonary retention of ultrafine and fine particles in rats. Am J Respir Cell Mol Biol **6**, 535–42.

30) Warheit DB, Hansen JF, Yuen IS, Kelly DP, Snajdr SI, Hartsky MA (1997) Inhalation of high concentrations of low toxicity dusts in rats results in impaired pul-

monary clearance mechanisms and persistent inflammation. Toxicol Appl Pharmacol **145**, 10–22.
31) Viallat JR, Raybuad F, Passarel M, Boutin C (1986) Pleural migration of chrysotile fibers after intratracheal injection in rats. Arch Environ Health **41**, 282–6.
32) Suzuki Y, Kohyama N (1991) Translocation of inhaled asbestos fibers from the lung to other tissues. Am J Ind Med **19**, 701–4.
33) Miller BE, Hook GER (1990) Hypertrophy and hyperplasia of alveolar type II cells in response to silica and other pulmonary toxicants. Environ Health Perspect **85**, 15–23.
34) Jensen CG, Jensen LCW, Rieder CL, Cole RW, Ault JG (1996) Long crocidolite asbestos fibers cause polyploidy by sterically blocking cytokinesis. Carcinogenesis **17**, 2013–21.
35) Gross KB, White HJ, Smiler KL (1984) Functional and morphologic changes in the lungs after a single intratracheal instillation of silica. Am Rev Respir Dis **129**, 833–9.
36) Porter DW, Hubbs A, Mercer R, Robinson VA, Ramsey D, McLaurin J, Khan A, Battelli L, Brumbaugh K, Teass A, Castranova V (2004) Progression of lung inflammation and damage in rats after cessation of silica inhalation. Toxicol Sci **79**, 370–80.
37) Morrow PE (1988) Possible mechanisms to explain dust overloading of the lungs. Fundam Appl Toxicol **10**, 369–84.
38) Oberdörster G (1995) Lung particle overload: implications for occupational exposures to particles. Regul Toxicol Pharmacol **27**, 123–35.
39) Driscoll KE, Costa DL, Hatch G, Henderson R, Oberdörster G, Salem H, Schlesinger B (2000) Intratracheal instillation as an exposure technique for the evaluation of respiratory tract toxicity: uses and limitations. Toxicol Sci **55**, 123–35.
40) Drew RT, Kuschner M, Bernstein DM (1987) The chronic effects of exposure of rats to sized glass fibers. Ann Occup Hyg **31**, 711–29.
41) Mauderly JL, Tesarek JE, Sifford LJ, Sifford LJ (1979) Respiratory measurements of unsedated small laboratory mammals using nonrebreathing valves. Lab Anim Sci **29**, 323–9.
42) Leong BK, Sabaitis CP, Rop DA and Aaron CS (1998) Quantitative morphometric analysis of pulmonary deposition of aerosol particles inhaled via intratracheal nebulization, intratracheal instillation or nose-only inhalation in rats. J Appl Toxicol **18**, 149–60.
43) Occupational Safety and Health Administration (2006) Regulation (Standards–29 CFR). Part 1910, occupational safety and health standards. Toxic and hazardous substances. Table Z-1 Limits for air contaminants. OSHA, Washington, DC. http://www.osha.gov/pls/oshaweb/owadisp.show_document?p_table=STANDARDS&p_id=9992#. Accessed July 21, 2009.
44) Maynard AD, Baron PA, Foley M, Shvedova AA, Kisin ER, Castranova V (2004) Exposure to carbon nanotube material: aerosol release during the handling of unrefined single-walled carbon nanotube material. J Toxicol Environ Health, Part A **67**, 87–107.
45) Galer DM, Leung HW, Sussman RG, Trzos RJ (1992) Scientific and practical considerations for the development of occupational exposure limits (OELs) for chemical substances. Regul Toxicol Pharmacol **15**, 291–306.
46) International Commission on Radiological Protection (2002) Reference values for regional deposition. In: Annals of the ICRP. ICRP supporting guidance 3. Guide for the practical application of the ICRP human respiratory tract model, Valentin J (Ed.), 91–2, Pergamon (Elsevier), Oxford.
47) Pinkerton KE, Gehr P, Crapo JD (1991) Architecture and cellular compositiom of the air-blood barrier. In: Treatise on pulmonary toxicology. Vol. 1. Comparative biology of the normal lung, Parent RA (Ed.), 121–8. CRC Press, Boca Raton.

J Occup Health 2010; 52: 155–166

Journal of Occupational Health

Genotoxicity and Cytotoxicity of Multi-wall Carbon Nanotubes in Cultured Chinese Hamster Lung Cells in Comparison with Chrysotile A Fibers

Masumi ASAKURA[1], Toshiaki SASAKI[1], Toshie SUGIYAMA[1], Mitsutoshi TAKAYA[2], Shigeki KODA[2], Kasuke NAGANO[1], Heihachiro ARITO[1] and Shoji FUKUSHIMA[1]

[1]Japan Bioassay Research Center, Japan Industrial Safety and Health Association and [2]National Institute of Occupational Safety and Health, Japan

Abstract: Genotoxicity and Cytotoxicity of Multi-wall Carbon Nanotubes in Cultured Chinese Hamster Lung Cells in Comparison with Chrysotile A Fibers: Masumi ASAKURA, *et al.* Japan Bioassay Research Center, Japan Industrial Safety and Health Association—Objectives: The potential applications and industrial production of multi-wall carbon nanotubes (MWCNT) have raised serious concerns about their safety for human health and the environment. The present study was designed to examine the *in vitro* cytotoxicity and genotoxicity of MWCNT and UICC chrysotile A (chrysotile). **Methods:** Cytotoxicity using both colony formation and lactate dehydrogenase (LDH) assays and genotoxicity including chromosome aberration, micronucleus induction and *hgprt* mutagenicity were examined by exposing cultured Chinese hamster lung (CHL/IU) cells to MWCNT or chrysotile at different concentrations. **Results:** The *in vitro* cytotoxicity of MWCNT depended on the solvent used for suspension of MWCNT and ultrasonication duration of the MWCNT suspension. A combination of DMSO/culture medium and 3-minute ultrasonication resulted in a well-dispersed medium with dispersion and isolation of agglomerated MWCNT by ultrasonication which manifested the highest cytotoxicity. The cytotoxicity was more potent for chrysotile than MWCNT. The genotoxicity of MWCNT was characterized by the formation of polyploidy without structural chromosome aberration, and an increased number of bi- and multi-nucleated cells without micronucleus induction, as well as negative *hgprt* mutagenicity. Chrysotile exhibited essentially the same genotoxicity as MWCNT, except for marginal but significant induction of micronuclei. MWCNT and chrysotile were incompletely internalized in the cells and localized in the cytoplasm. **Conclusions:** MWCNT and chrysotile were cytotoxic and genotoxic in Chinese hamster lung cells, but might interact indirectly with DNA. The results suggest that both test substances interfere physically with biological processes during cytokinesis.
(J Occup Health 2010; 52: 155–166)

Key words: Asbestos, Chinese hamster lung cell, Cytotoxicity, Genotoxicity, Multi-wall carbon nanotube, Polyploidy

Carbon nanotubes (CNT) forming a cylinder of one or several graphite layers are termed single-wall carbon nanotubes (SWCNT) or multi-wall carbon nanotubes (MWCNT), respectively. Since CNT exhibits outstanding physicochemical and mechanical properties such as high tensile strength, ultra-light weight, thermal and chemical stability, as well as excellent semi-conductive electronic properties, this nanomaterial is expected to have many applications in various sectors of industry such as electronics, construction, aerospace, chemicals, pharmaceuticals and medicine[1)]. Annual production volumes of SWCNT and MWCNT in Japan were estimated to be 0.1 and 60 tons in 2008, respectively[2)]. The potential applications and industrial production of SWCNT and MWCNT have raised concerns about their safety for human health and the environment. In particular, workers might be at high health risk of excessive exposure to CNT during its handling. Han *et al.*[3)] reported that workers were exposed to 0.33 mg/m^3 in a MWCNT-manufacturing process as measured with a personal sampling device. No epidemiological or medical

Received Nov 24, 2009; Accepted Feb 15, 2010
Published online in J-STAGE Apr 2, 2010
Correspondence to: M. Asakura, Japan Bioassay Research Center, Japan Industrial Safety and Health Association, 2445 Hirasawa, Hadano, Kanagawa 257-0015, Japan
(e-mail: m-asakura@jisha.or.jp)

case studies have been reported on the health outcomes of CNT-exposed workers. Although the toxicity of CNT has been studied both *in vivo* and *in vitro*, there is a paucity of toxicity and carcinogenicity data available for the health risk assessment of workers exposed to CNT. Recently, induction of mesotheliomas by intraperitoneal and intrascrotal injections of straight type MWCNT in p53 gene-deficient mice[4)] and male F344 rats[5)], respectively, and asbestos-like pathogenicity by intraperitoneal injection of MWCNT in female mice[6)] have been reported. Mutation of the k-*ras* gene locus in the lungs of mice exposed by inhalation to SWCNT[7)] and positive clastogenicity and aneugenicity of MWCNT[8)] in Type II pneumocytes of female rats intratracheally instilled with MWCNT are also noteworthy. *In vitro* cytotoxicity studies using SWCNT and MWCNT have revealed varying degrees of cytotoxicity depending on physical dimensions such as length and width, agglomerated or dispersed state, functionalization and metal impurities[9–20)]. *In vitro* genotoxicity studies have demonstrated that SWCNT and MWCNT showed genotoxicity in a micronucleus assay[8)] and in a mutation assay with mouse embryonic stem cells[20)], although bacterial mutagenicity was not shown for these nanomaterials[22–24)].

Recent *in vivo*[4–6)] and *in vitro*[11–13)] toxicity studies have suggested that the hazardous effects of MWCNT fibers resemble those of asbestos fibers, because of the similarity in physical dimensions and biopersistence of MWCNT and asbestos[25)]. The present study was designed to examine the cytotoxicity and genotoxicity of MWCNT, including chromosome aberration, micronucleus induction, and mutagenicity at the hypoxanthine-guanine phosphoribosyltransferase (*hgprt*) locus, as well as scanning electron microscopic (SEM) and light-microscopic observations of MWCNT-exposed cells, in an *in vitro* study using a Chinese hamster lung (CHL/IU) cell line and therefore to compare the cytotoxicity and genotoxicity of MWCNT with those of UICC chrysotile A (chrysotile) asbestos.

Materials and Methods

Chemicals

MWCNT was donated by MITSUI & Co. Ltd. (MWNT-7, Lot No. 061220, Tokyo, Japan). It was found in our previous study[26)] that the mean and SD of the fiber lengths were 5.0 ± 4.5 μm for MWCNT. Fibers longer than 5 μm were found to occupy 38.9% of the total fibers counted, and the mean and SD of the fiber widths were 88 ± 5 nm, resulting in an average ratio of 57. Chrysotile A of UICC (Union Internationale Contre le Cancer) was donated by Dr. M. Kudo, Occupational Health Research and Development Center, Japan Industrial Safety and Health Association. The length distribution of UICC chrysotile A was reported to be 20.7, 34.9, 23.1 and 15.2% for 0.2–0.5, 0.5–1.0, 1–2 and 2–5 μm, respectively[27)], indicating that the distribution of fiber lengths in chrysotile was skewed apparently to shorter lengths than that in MWCNT. MWCNT and chrysotile were used without being purified or further sieved. It was also found in the previous study[26)] that MWCNT contained 4,400 ppm (wt/wt) iron, 48 ppm chromium and 17 ppm nickel by graphite furnace atomic absorption spectrometric analysis. Eagle's MEM was purchased from GIBCO (Invitrogen Cell Culture, CA, USA), calf serum (CS) from JRH Biosciences (Kansas City, USA). Carboxymethyl cellulose sodium salt (CMC), dimethylsulfoxide (DMSO) and polyoxyethylene (20) sorbitan monooleate (Tween 80) were purchased from Wako Pure Chemical Industries, Ltd. (Osaka, Japan). Phosphate-buffered saline (PBS) was purchased from Nissui Pharmaceutical Co. Ltd. (Tokyo, Japan). Mitomycin C (MMC) and ethyl methanesulfonate (EMS) used as positive controls were purchased from Wako Pure Chemical Industries, Ltd. (Osaka, Japan). Ultra-pure water was manufactured in-house with a water purification system (Milli-Q synthesis A10, Millipore Corporation, MA, USA).

Suspension and dispersion of MWCNT or chrysotile in solvent

Since MWCNT is water-insoluble and is agglomerated firmly to micron-sized particles, it must be suspended in an appropriate solvent and dispersed into isolated fibers by ultrasonication. The most suitable solvent was selected from the following 4 solvents, in combination with the 3-minute ultrasonication. 1) Direct suspension of MWCNT in Eagle's MEM supplemented with 10% heat-inactivated CS used as culture medium. 2) Suspension of MWCNT in a mixture of DMSO and the culture medium with a final concentration of DMSO in the culture medium suspending MWCNT of 0.5% (5.5 mg/m*l*; 70 mM). 3) Suspension of MWCNT in an aqueous solution containing Tween 80 followed by addition of the ultrasonicated suspension into the culture medium. The final concentration of Tween 80 in the culture medium suspending MWCNT was 0.1 mg/m*l*. 4) Suspension of MWCNT in CMC solution followed by addition of the ultrasonicated suspension into the culture medium. The final concentration of CMC in the culture medium suspending MWCNT was 1 mg/m*l*. All these solvents displayed no cytotoxicity in the range of the concentrations used here. Since in our preliminary experiment chrysotile was found to be wettable in water, chrysotile was suspended in ultra-pure water (milli-Q). This was added to the culture medium at final concentrations of 0.25 to 50 μg/m*l* and ultrasonicated for 3 min. An ultrasonic homogenizer (VP-30S, 20 kHz, 300 W, TAITEC Co. Ltd., Tokyo, Japan) was used to ultrasonicate the suspensions of MWCNT or chrysotile. The time period of 3 min for the ultrasonication was determined from the empirical relationship between the time periods of ultrasonication and dispersion of MWCNT as indicated by the size distribution of MWCNT in the DMSO/culture medium. A dynamic light scattering size (DLS) apparatus, Zetasizer Nano DLS Analyzer (Malvern, Worcestershire, UK), was used to measure the size distribution of MWCNT in the suspension. The vertical axis of intensity against hydrodynamic diameters, shown in Fig. 1A and 1B, represents the normalized intensity of the light scattered through the aqueous media containing MWCNT, and was expressed as a percentage of total intensity (total area as 100%). The normalized intensity of scattered light depends on both the number of particles and their sizes.

Cells

A clonal sub-line derived from the lung of a newborn female Chinese hamster (CHL/IU) was donated by the National Institute of Health Sciences (Tokyo, Japan). The cells were cultured in Eagle's MEM supplemented with 10% heat-inactivated CS (culture medium), and grown in a monolayer. The modal chromosome number was 25 and the doubling time was approximately 15 h[28].

Colony formation assay for cytotoxicity

One hundred cells (20 cells/m*l* × 5 m*l*) of single cell suspension were seeded in a 60-mm plastic culture dish, incubated in a culture medium for 24 h, and then replaced with the test substance suspended in culture medium. The cells were exposed to MWCNT at 12.5 to 400 μg/m*l* or chrysotile at 0.25 to 50 μg/m*l* for 7 days. Then, the cells were fixed with ethanol for 5 min and stained with 0.1% crystalviolet for 20 min, and colonies were counted under a microscope. The percentage of surviving cells (viability) was calculated by dividing the number of colonies formed during MWCNT treatment by the number of colonies in the control medium and multiplying by 100.

Lactate dehydrogenase (LDH) assay for cytotoxicity

One hundred thousand cells (20,000 cells/m*l* × 5 m*l*) were seeded in a 60-mm plastic culture dish, incubated in a culture medium for 48 h, and then replaced with the test substance suspended in culture medium. The cells were exposed to MWCNT at 12.5 to 400 μg/m*l* or chrysotile at 10 μg/m*l* for 24 h. The medium containing the test substance was then centrifuged at 13,000 rpm (16,000 × g) for 5 min. The LDH concentration in the supernatant was measured by a Clinical Analyzer (7070, Hitachi, Ltd. Tokyo, Japan). The remaining cells in the dish were transferred to a 0.1% tritonX-100 solution to extract LDH inside the cells, and then centrifuged at 13,000 rpm for 5 min. The LDH concentration in the supernatant was measured by the same method as described above. The LDH release rate was calculated by dividing the concentration of LDH in the test substance

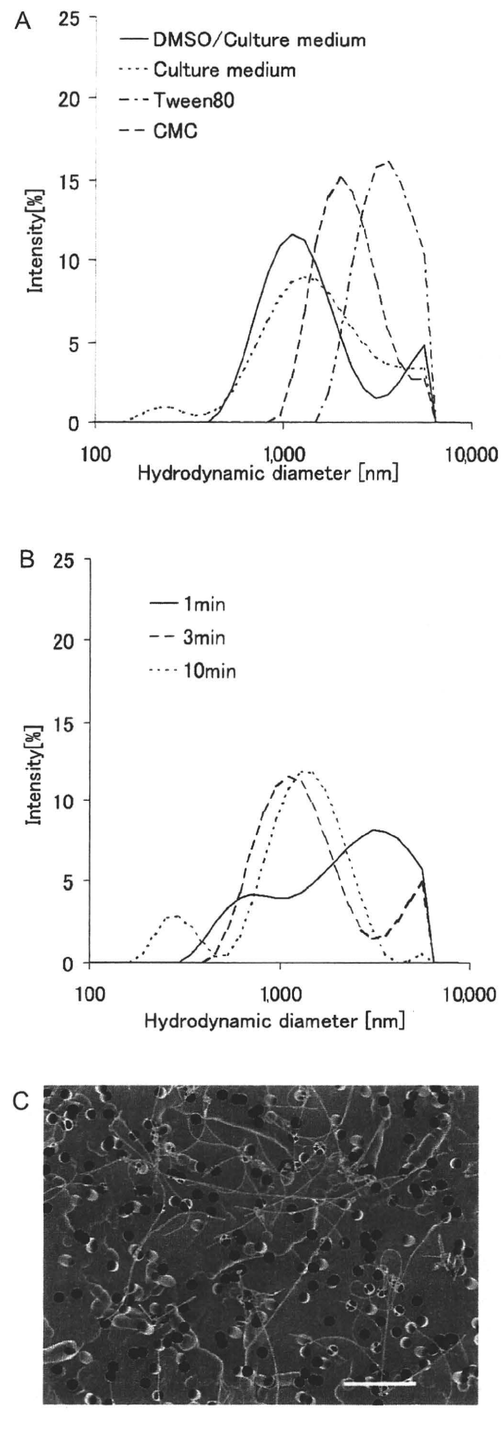

Fig. 1. Size distribution curves of MWCNT suspended in various solvents (A) and in DMSO/culture medium ultrasonicated for different durations with an ultrasonic homogenizer (B). A SEM image (C) showing good dispersion of agglomerated MWCNT into single, isolated fibers in the DMSO/culture medium after 3 min ultrasonication. Bar indicates 5 μm.

suspended in culture medium by the total concentration of LDH inside (in the triton X-100 solution) and outside the cells and multiplying by 100.

Chromosome aberration assay

One hundred thousand cells (20,000 cells/ml × 5 ml) were seeded in a 60-mm plastic culture dish, incubated in a culture medium for 24 h, and then replaced with test substance suspended in culture medium. The cells were exposed to MWCNT at 0.078 to 80 μg/ml or chrysotile at 0.8 to 20 μg/ml for 24 or 48 h. DMSO at 0.5% or ultra-pure water at 5% served as a negative control and MMC at 0.04 μg/ml as a positive control. Treatment concentrations of MWCNT or chrysotile were determined on the basis of the preliminary chromosome aberration assay. For chromosome preparation, colcemid at a final concentration of 0.2 μg/ml was added to the culture medium 2 h before cell harvesting. Chromosomes were prepared by the air-drying method and stained with 2% Giemsa. The cytotoxicity was assessed by counting the trypan blue-stained cells as the dead ones, and expressed as a growth index by dividing the number of viable cells after 24- or 48-hour treatment with MWCNT or chrysotile by that of the respective negative control. The frequency of the cells with various types of structural aberrations including chromatid break, chromatid exchange, chromosome break, chromosome exchange and others (fragmentations except pulverization), for each dose in a 200 well-spread metaphase (100 metaphase/culture), as well as the cells with numerical aberration (polyploidy) were scored.

Micronucleus assay

Twenty-four thousand cells (12,000 cells/ml × 2 ml) were seeded in a 35-mm plastic culture dish, incubated in a culture medium for 24 h, and then replaced with the test substance suspended in culture medium. The cells were exposed to MWCNT at 0.02 to 5.0 μg/ml or chrysotile at 0.1 to 1.6 μg/ml for 48 h. DMSO at 0.5% or ultra-pure water at 5% served as a negative control and MMC at 0.01 μg/ml as a positive control. Treatment concentrations of MWCNT or chrysotile were determined on the basis of the preliminary micronucleus assay. The cells were washed with PBS, fixed with 10% formaline and stained by mounting with 40 μg/ml acridine orange and 10 μg/ml DAPI solution. Immediately after the staining, the cells were observed with fluorescence microscopy using blue excitation, and evaluated for the number of cells having micronuclei, bi-nuclei and multi-nuclei having more than two nuclei in 2,000 intact interphase cells (1,000 cells/culture). The cytotoxicity was expressed as a growth index by dividing the number of viable cells after the 48-hour treatment with MWCNT or chrysotile by that of the respective negative control. Micronucleus was defined as having less than one-fourth of the diameter of the main nucleus. Numbers of bi-nucleated cells and mitotic cells as well as multi-nucleated cells having more than two nuclei appearing in the same microscopic field were also counted.

Mutation assay at the hgprt locus

Three-hundred thousand cells (30,000 cells/ml × 10 ml) were seeded in a 100-mm plastic culture dish, incubated in a culture medium for 24 h, and then replaced with the test substance suspended in culture medium. The cells were exposed to MWCNT at 6.3 to 100 μg/ml or chrysotile at 1.56 to 25 μg/ml for 48 h. DMSO at 0.5% or ultra-pure water at 5% served as a negative control and EMS at 200 μg/ml as a positive control. Treatment concentrations of MWCNT or chrysotile were determined on the basis of the preliminary mutation assay. Then, the cells were rinsed with PBS and incubated in normal medium for a mutation expression time of 6 days. After the 6-day incubation, the cells were treated with trypsin, and 40,000 cells were transferred to each of twenty 60-mm culture dishes in medium containing 6-thioguanine (6-TG) for mutation selection. One hundred cells transferred to each of three 60-mm culture dishes in normal medium were used for cell viability assessment. After incubating for 10 days, the cell colonies formed were fixed with ethanol and stained with 5% Giemsa, and the number of 6-TG-resistant colonies was counted. The mutation frequency rate was expressed as the scored number of 6-TG-resistant cells per 10^6 cells corrected by the cell viability.

Light-microscopic and SEM observations of cells exposed to MWCNT or chrysotile and MWCNT in the suspension

The cells were exposed to MWCNT or chrysotile for 48 h. For light-microscopic observation, the cells exposed to MWCNT were fixed with methanol, and stained with 5% Giemsa. The chrysotile-exposed cells were fixed with methanol and observed under a phase-contrast microscope. For the SEM cell observation, the cells were pre-fixed in 1% glutaraldehyde in PBS, rinsed 4 times in PBS, and dehydrated using increasing concentrations of ethanol. After ethanol was replaced with *t*-butanol, the samples were subjected to critical point drying and sputter-coated with Pt. The cells and MWCNT or chrysotile were examined by SEM (SU-8000, Hitachi, Ltd., Tokyo, Japan). In order to examine whether MWCNT was dispersed in the culture medium, MWCNT was suspended in the DMSO/culture medium at 400 μg/ml and ultrasonicated for 3 min. Then, the suspension was diluted to 1/10 in the medium, dripped onto an Isopore Track-Etched membrane filter (Millipore, Bedford, USA) and dried. After the filter was sputter-coated with Pt, MWCNT was observed by SEM.

Statistical analysis

The statistical significance of the dose-response relationship was tested by the Cochran-Armitage test.

Fisher's exact test was used for statistical comparisons between data of the dosed-groups and the respective controls. *p* values of less than 0.05 were considered to be statistically significant. A positive response showing mutagenicity at the *hgprt* locus was judged as being biologically significant, when the mutation rate of the cells exposed to MWCNT or chrysotile was 2-fold greater than the negative control.

Results

Suspension and dispersion of MWCNT or chrysotile in solvent

In the present study, the distribution of hydrodynamic diameters of MWCNT in the suspension as assessed by the DLS measurement was used as an indicator of the MWCNT dispersion in the suspension. As shown in Fig. 1A, the principal peak was shifted toward smaller hydrodynamic diameters in the following order of the solvents: DMSO/culture medium>culture medium>CMC>Tween 80. This result indicates that MWCNT was dispersed more finely in DMSO/culture medium than in culture medium, CMC or Tween 80, when the ultrasonication duration was fixed at 3 minute. As shown in Fig. 1B, the 3- or 10-minute ultrasonication was found to decrease the hydrodynamic diameters of MWCNT more finely than the 1-minute ultrasonication. Besides, a small peak of 300 nm in the hydrodynamic diameter appeared after the 10-minute ultrasonication. A SEM image (Fig. 1C) revealed that MWNT was not agglomerated but dispersed into single, isolated fibers in the DMSO/culture medium after the 3-minute ultrasonication.

Cytotoxicity

Figure 2A shows the effects of solvents used for the MWCNT suspension on cytotoxicity as evaluated by a colony formation assay with CHL/IU cells. The cell viability decreased with an increase in dose levels of MWCNT for all the solvents, and the cell viability tended to decrease in the following order: DMSO/culture medium>culture medium>Tween 80>CMC. DMSO/culture medium exhibited the most potent cytotoxicity of MWCNT among the four solvents, suggesting that addition of DMSO to the culture medium (MEM+10% CS) helped to assure good dispersion of hydrophobic substances leading to potent toxicity. The dose-response curves of the cytotoxicities of chrysotile and MWCNT (Fig. 2A) revealed that the cytotoxicity of chrysotile was much more potent than that of MWCNT, when evaluated by the colony formation assay.

Figure 2B shows effect of ultrasonication duration on the cytotoxicity of MWCNT as evaluated by the colony formation assay. After 3-minute ultrasonication, MWCNT tended to exhibit more potent cytotoxicity at dose levels greater than 100 μg/m*l* than after 1- or 10-minute

A

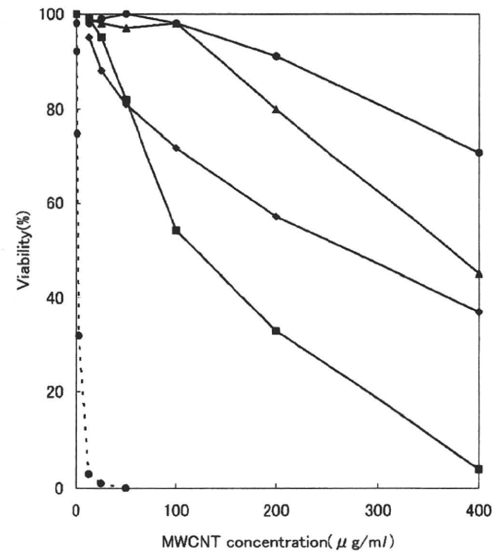

Effect of solvent used for MWCNT suspension on its cytotoxicity with CHL/IU cells. —◆— culture medium, —■— DMSO/culture medium, —▲— Tween 80, —●— 1%CMC, - ●-chrysotile (water).

B

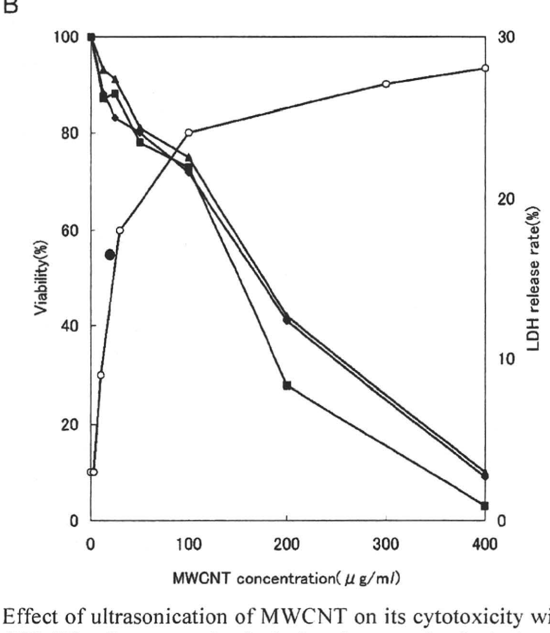

Effect of ultrasonication of MWCNT on its cytotoxicity with CHL/IU cells. —◆— 1 min (colony), —■— 3 min (colony), —▲— 10 min (colony), —○— 3 min (LDH), ● : LDH release rate of chrysotile at 10μg/m*l*.

Fig. 2. Dose-response curves of cytotoxicity induced by MWCNT suspended in various solvents and chrysotile in a colony formation assay (A), and of cytotoxicity induced by MWCNT ultrasonicated for different duration in a colony formation assay together with the dose-response curve of LDH release rate induced by MWCNT (B). The LDH release rate of chrysotile at 10 μg/m*l* is indicated by a closed circle.

Table 1. Structural and numerical chromosome aberrations of MWCNT and chrysotile with CHL/IU cells

Treatment time (h)	Concentration (μg/ml)	Percent (%) of cells showing structural chromosome aberrations							Percent (%) of cells showing polyploids		Growth index (%)
		Cell No.	ctb	cte	csb	cse	other	total	Cell No.	polyploidy	
MWCNT											
	0	200	0	0	0	0	0	0	201	0.5	100
	1.3	200	0	0	0	0	0	0	203	1.5	76
	5.0	200	0	0	0	0	0	0	207	3.4*	62
24	20	200	0	0	0	0	0	0	234	14.5**	56
	80	200	0	0	0	0	0	0	242	17.4**	50
								ns[a]		$p<0.01$[a]	
	MMC	200	7	23.5	0	0	0	28.5**	200	0	–
	0	200	0.5	0	0	0	0	0.5	202	1.0	100
	0.078	200	0.5	0	0	0	0	0.5	203	1.5	83
	0.31	200	0.5	0	0	0	0	0.5	204	2.0	74
48	1.3	200	0	0	0	0	0	0	217	7.8**	67
	5.0	200	0	0	0	0	0	0	261	23.4**	59
								ns[a]		$p<0.01$[a]	
	MMC	200	6.5	58.5	0	0	0	63**	200	0	–
Chrysotile											
	0	200	0	1.5	0.5	0	0	2.0	201	0.5	100
	0.8	200	0.5	0.5	0	0	0	1.0	209	4.3*	80
4	4.0	200	0.5	1.5	0	0	0	2.0	258	22.5**	69
	20	200	0	0	0	0	0	0	304	34.2**	42
								ns[a]		$p<0.01$[a]	
	MMC	200	11	30	0	0	0	38.5**	201	0.5	–
	0	200	0.5	0	0	0	0	0.5	201	0.5	100
	0.8	200	0.5	0.5	0	0	0	1.0	208	3.8*	96
48	4.0	200	1.0	1.0	0	0.5	0	2.5	224	10.7**	81
	20	200	1.0	0.5	0	0.5	0	2.0	330	39.4**	42
								ns[a]		$p<0.01$[a]	
	MMC	200	13	35.5	0	0.5	0	41.5**	201	0.5	–

Fisher's exact test: * $p<0.05$, ** $p<0.01$. a) Cochran-Armitage test. ctb: chromatid break; cte: chromatid exchange; csb: chromosome break; cse: chromosome exchange; others: fragmentation etc. (except pulverization); MMC: Mitomycin C at 0.04 μg/ml.

ultrasonication. On the basis of this result, the time period for ultrasonication of the MWCNT suspension was fixed at 3 min throughout the present study. Figure 2B also shows that both colony formation and LDH assays exhibited clear but different dose-response curves for cytotoxicity. It was also found that the LDH release rate of chrysotile at 10 μg/ml was greater than that expected from the dose-response curve of MWCNT, indicating that chrysotile damaged the CHL/IU cells more severely than MWCNT on an equal mass basis.

Chromosome aberration

As shown in Table 1, neither MWCNT nor chrysotile induced any type of structural chromosome aberrations for the 24- or 48-hour continuous treatment at the designated dose levels. On the other hand, both MWCNT and chrysotile induced numerical chromosome aberrations of polyploidy in a significantly dose-dependent manner as indicated by the Cochran-Armitage test. A significantly increased number of cells showing polyploidy was observed for MWCNT at 5 μg/ml and above in the 24-hour treatment and at 1.3 and 5 μg/ml in the 48-hour treatment. Chrysotile significantly induced higher polyploidy at lower dose levels than MWCNT did on an equal mass basis. The minimum dose levels of MWCNT and chrysotile for the significant induction of